Ballistic-like space-charge-limited currents in halide perovskites at room temperature

Osbel Almora, Daniel Miravet, Marisé García-Batlle, et al.

Ballistic-like space-charge-limited currents in halide perovskites at room temperature

View Online   Export Citation   CrossMark

Osbel Almora,[1,2,a] (iD) Daniel Miravet,[3] (iD) Marisé García-Batlle,[1] (iD) and Germà Garcia-Belmonte[1] (iD)

AFFILIATIONS

[1]Institute of Advanced Materials (INAM), Universitat Jaume I (UJI), 12006 Castelló, Spain

[2]Erlangen Graduate School of Advanced Optical Technologies (SAOT), Friedrich-Alexander Universität Erlangen-Nürnberg, 91052 Erlangen, Germany

[3]Quantum Theory Group, Department of Physics, University of Ottawa, Ottawa K1N 7N9, Canada

[a]Author to whom correspondence should be addressed: almora@uji.es

ABSTRACT

The emergence of halide perovskites in photovoltaics has diversified the research on this material family and extended their application toward several fields in the optoelectronics, such as photo- and ionizing-radiation-detectors. One of the most basic characterization protocols consists of measuring the dark current–voltage ($J - V$) curve of symmetrically contacted samples for identifying the different regimes of the space-charge-limited current (SCLC). Customarily, $J \propto V^n$ indicates the Mott–Gurney law when $n \approx 2$ or the Child–Langmuir ballistic regime of SCLC when $n = 3/2$. The latter has been found in perovskite samples. Herein, we start by discussing the interpretation of $J \propto V^{3/2}$ in relation to the masking effect of the dual electronic–ionic conductivity in halide perovskites. However, we do not discard the actual occurrence of SCLC transport with ballistic-like trends. Therefore, we introduce the models of quasi-ballistic velocity-dependent dissipation (QvD) and the ballistic-like voltage-dependent mobility (BVM) regimes of SCLC. The QvD model is shown to better describe electronic kinetics, whereas the BVM model results are suitable for describing both electronic and ionic kinetics in halide perovskites as a particular case of the Poole–Frenkel ionized-trap-assisted transport. The proposed formulations can be used as the characterization of effective mobilities, charge carrier concentrations and times-of-flight from J–V curves, and resistance from impedance spectroscopy spectra.

Halide perovskites, e.g., methylammonium lead triiodide (MAPbI$_3$), have emerged as one of the most attractive material families for optoelectronic applications, such as photovoltaics,[1] ionizing radiation detectors,[2] field-effect transistors,[3] memristors,[4] and energy storage.[5] The reason for that is the optimal properties for photon absorption and charge transport as well as the easy solution-based fabrication methods, which has motivated intensive research. At a material level, one of the most basic and commonly performed characterization techniques is the current density–voltage (J–V) measurement, which can inform on the transport mechanisms and properties. Notably, the study of the dark J–V curves of halide perovskites results are particularly puzzling due to the dual ionic-electronic conductivity of these materials, resulting in many artifacts and anomalous behaviors, typically known as the J–V hysteresis effect.

The main transport mechanisms usually reported in symmetrically contacted samples (no built-in voltages V_{bi} at the electrodes) of hybrid perovskites are the Ohmic and the space-charge-limited current (SCLC). In the Ohmic regime, the current and the electrostatic potential (φ) are linear with the applied voltage and the position (x), respectively [see Figs. 1(a) and 1(b)]. Differently, in the SCLC regime, the current may deviate from the linear behavior due to significant modification in the charge density profile as the electric field increases with the externally applied voltage.

The most common form of SCLC is that of the mobility regime, where the current follows the Mott–Gurney law ($J \propto V^2$).[6,7] Within this regime, one can often find the trap-filling ($J \propto V^{>2}$) sub-regime,[8] which allows the estimation of the concentration of deep level trap defects.[7] Subsequently, upon high enough injection of charge carriers, the velocity saturation regime ($J \propto V$)[9,10] takes place. These regimes are well known, and their identification in hybrid halide perovskites is generally not questioned with the classic distribution of Fig. 1(a).

Another fundamentally different SCLC regime is that of the ballistic transport, as the Child–Langmuir law,[11,12] where
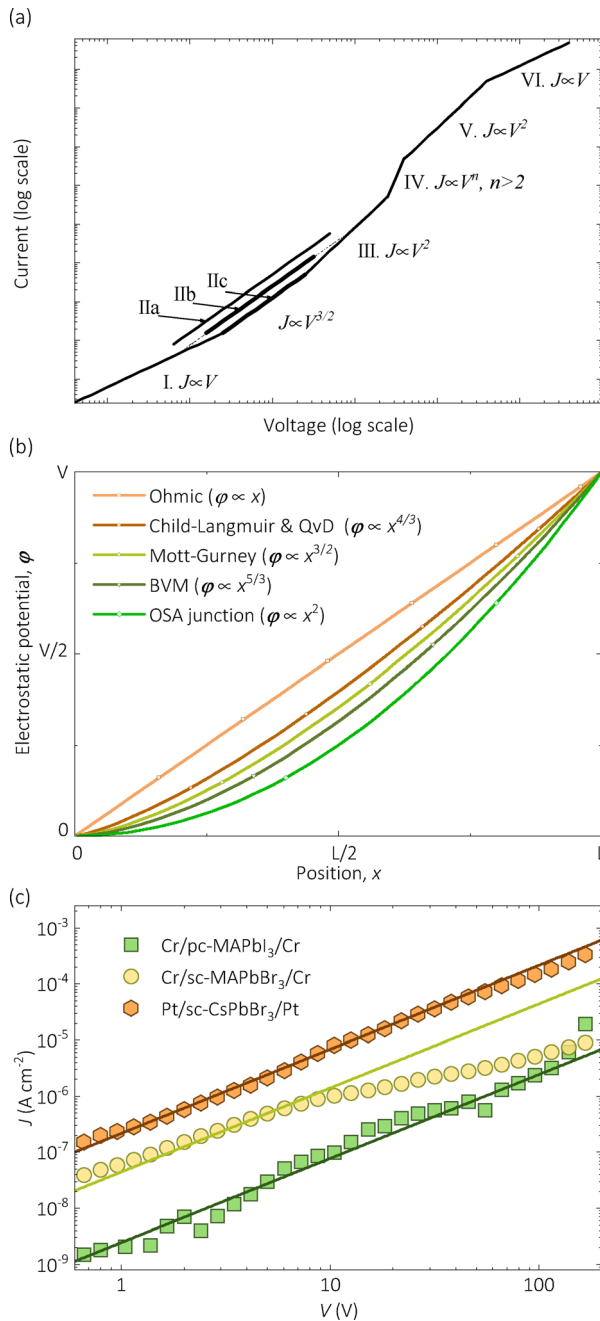
FIG. 1. Current density as a function of the external applied voltage. (a) Theoretical transport regimes: (I) Ohmic, (IIa) ballistic Child-Langmuir law[11,12] of SCLC, (IIb) quasi-ballistic velocity-dependent dissipation (QvD) model of SCLC, (IIc) ballistic-like voltage-dependent mobility (BVM) model of SCLC, (III) Mott–Gurney law[7] trap-empty SCLC, (IV) trap filling,[7] (V) Mott–Gurney law trap-filled,[7] and (VI) velocity saturation.[7] (b) Electrostatic potential as a function of position between electrodes separated a distance L upon application of voltage V for several configurations from Ohmic to one-sided abrupt (OSA) junction, as indicated. (c) Experimental curves from various perovskite samples (dots) reported in the supplementary material of our simultaneous works,[19,21] licensed under Creative Commons Attribution Noncommercial (CC-BY-NC) licenses, and allometric fitting (lines) to the ballistic-like behavior ($J \propto V^{3/2}$).

$$J = \frac{4\epsilon_0\epsilon_r}{9\,L^2}\sqrt{\frac{2Q}{M}}V^{3/2}. \qquad (1)$$

Here, ϵ_0 is the vacuum permittivity; ϵ_r is the dielectric constant; L is the distance between electrodes; and Q and M are the charge and the effective mass of the charge carriers, respectively. In physical terms, unlike the mobility regime, in the ballistic regime, no scattering is considered (the definition of mobility is not justified), and the maximum drift velocity results,

$$v_d = \sqrt{\frac{2Q}{M}}V, \qquad (2)$$

as a consequence of the conservative transformation of electrostatic energy into kinetic energy. This model was initially thought for vacuum conditions, and among semiconductors, it has been considered for either low temperature conditions,[13] short enough distance,[14] or timescale (near-ballistic regime).[15] Notably, in practice, with typical measurement conditions ($V \le 100$ V, room temperature $T \sim 300$ K, electrode active area A > 0.01 cm^2, $\epsilon_r = 23$[16]), the ballistic currents of MAPbI$_3$ samples would result significantly high for $L < 10\,\mu$m (e.g., $J > 10$ A cm^{-2} at 10 V), as presented in Fig. S1 in the supplementary material. In addition, if present, a bulk mechanism, such as the SCLC, is commonly overlapped by interface phenomena in thin film samples where the distance between electrodes is on the order of the diffusion and/or Debye lengths. Therefore, it makes sense to discard Child–Langmuir's ballistic SCLC transport as a major mechanism for operational currents in thin film samples.

In thick halide perovskite samples, the SCLC regimes with trends $J \propto V^n$ and $1 < n < 2$ have been identified,[17] which may suggest the presence of some sort of ballistic-like transport. For example, Fig. 1(c) shows three different perovskite samples showing some section of the dark J–V curve with $n \approx 3/2$, characterized in our previous and simultaneous works and measured in room conditions with a Keithley Source-meter 2612B.[18,19] The chromium contacted 1-mm-thick polycrystalline (pc) pellet (Cr/pc-MAPbI$_3$/Cr)[18] reports the lower currents, and the 2 mm-thick single crystal (sc) of the CH$_3$NH$_3$PbBr$_3$ (Cr/sc-MAPbBr$_3$/Cr)[20] sample presents the shorter voltage section with the $J \propto V^{3/2}$ trend, whereas the platinum contacted 3 mm-thick CsPbBr$_3$ sample (Pt/sc-CsPbBr$_3$/Pt)[19] seems to behave the closest to the seemly ballistic comportment.

In this Letter, first, we question the identification of the ballistic regime of SCLC in hybrid halide perovskite and analyze possible misleading influences of the ionic–electronic character of the conductivity in these materials. Second, we provide analytical formulations in two models that reproduce a similar behavior ($J \propto V^{3/2}$) despite not being strictly ballistic regimes: the quasi-ballistic velocity-dependent dissipation (QvD) and the ballistic-like voltage-dependent mobility (BVM) regime of SCLC.

For all SCLC regimes, any trend from a dark J–V curve of halide perovskite samples should be taken with cautions, because of the hysteresis issues. For instance, Duijnstee et al.[22,23] recently suggested the use of temperature-dependent-pulsed-voltage-SCLC measurements as a validating technique for ensuring the identification of one or another transport regime. Also, Alvar et al.[24] showed that how the frequency dependence of the permittivity of thin film perovskites and their dependence on the voltage scan rate and temperature influence the analysis of the SCLC. Moreover, the temperature-modulated-SCLC

spectroscopy study of Pospisil et al.[25] found multicomponent deep trap states in pure perovskite crystals, assumingly caused by the formation of nanodomains due to the presence of the mobile species in the perovskites. These and more studies suggest that any claim of SCLC from J–V curves should be double checked for hysteresis or ion migration related artifacts, before extracting parameters. For instance, the J–V curves of Fig. 1(c) were not reproducible when long periods of pre-biasing preceded the voltage sweeps.

Regarding the classic ballistic regime of SCLC in halide perovskites, even if a $J \propto V^{3/2}$ trend is validated as hysteresis-free, there is little likelihood for the mechanism to be present at room temperatures. On the one hand, the condition of negligible energy dissipation for charge carriers is arguably unrealistic for transport from one electrode to the other, regardless whether they are electronic or ionic charge carriers. Notably, even though there is evidence of ballistic transport lengths $\sim$200 nm in MAPbI$_3$ thin films, it has been reported in a timescale of 10–300 fs.[26–28] On the other hand, a fair assumption would be for the $J \propto V^{3/2}$ tendency to more likely be an intermediate sub-regime of transition between the Ohmic regime ($J \propto V$) and the mobility regime ($J \propto V^{\geq 2}$), or between this latter and Ohmic-seemly velocity saturation regime ($J \propto V$). However, a $J \propto V^{3/2}$ behavior could occur in a way that resembles the SCLC ballistic mechanism at room temperature. For this to happen in the SCLC formalism, two main scenarios can be considered. First, a quasi-ballistic SCLC transport can occur in the case of an energy dissipation proportional to the velocity, resembling that due to Stokes's drag dissipation forces. Second, a ballistic-like SCLC transport takes place due to a behavior of $v_d \propto V^{1/2}$ not related at all with energy conservation (ballistic regime) but with a bias-dependent energy dissipation (mobility regime).

The core of the deduction of the classic SCLC resides in neglecting the diffusion currents (div $\mathbf{J} = 0$) and assuming that the total current density is mostly the drift component with a given relation between v_d and the electrostatic potential φ or the absolute value of the electric field $|\xi| = |d\varphi/dx|$. Mathematically, for a sample with distance L between electrodes at an external voltage V and $v_d \propto \varphi^p$, one can always find a solution of the Poisson equation with a position-independent current, such as $J = K\, V^{p+1} L^{-2}$, where K is a constant (see Eq. (S10) in Sec. S1 of the supplementary material). Thus, $v_d \propto \varphi^{1/2}$ results in the Child–Langmuir ($J \propto V^{3/2}$)[11,12] law with a potential $\varphi \propto x^{4/3}$ (see Fig. 1).

Unlike the classic ballistic approach, where all the electrostatic energy is converted into kinetic energy, a dissipation term is included as a correction in the QvD model. The energy dissipated during the transport of the charge carrier from one electrode to the other is considered in the form of $W = M\nu L v_d$, similarly to a Stokes's drag dissipation mechanism. Here, the momentum relaxation rate as $\nu = \nu_0(\varphi/V_0)^{1/2}$ is such that it agrees with Teitel and Wilkins' conditions for the typical v_d time overshoot, as previously considered for near-ballistic transport in one-valley semiconductors.[29] The characteristic dissipation frequency ν_0 is on the order of the black-body radiation and ν increases with the potential, thus V, over the threshold value V_0, attaining a maximum at the biased electrode. Moreover, V_0 is also expected to relate to L balancing the dissipation energy in a form that W only depends on the position x through φ and v_d. Subsequently, the energy conservation results as

$$\frac{M}{2}v_d^2 + \sqrt{\beta MQ\varphi}\,v_d = Q\varphi, \tag{3a}$$

where the dimensionless QvD coefficient is

$$\beta = \frac{M\nu_0\mu_\beta}{Q}, \tag{3b}$$

and the effective mobility is $\mu_\beta = \nu_0 L^2/V_0$. Notably, the use of effective mobilities has been earlier introduced in quasi-ballistic transport in high electron mobility transistors.[30] In Fig. 2(a), the typical values for β as function of ν_0 and μ_β for a charge carrier with the elementary charge q and the electron mass m_e. The exact solution of Eq. (3) is only different to (2) by a factor $((2+\beta)^{1/2} \pm \beta^{1/2})$, which is $2^{1/2}$ in the limit of $\beta \to 0$. Note that the solution with the plus must be discarded because the dissipation cannot increase the velocity.
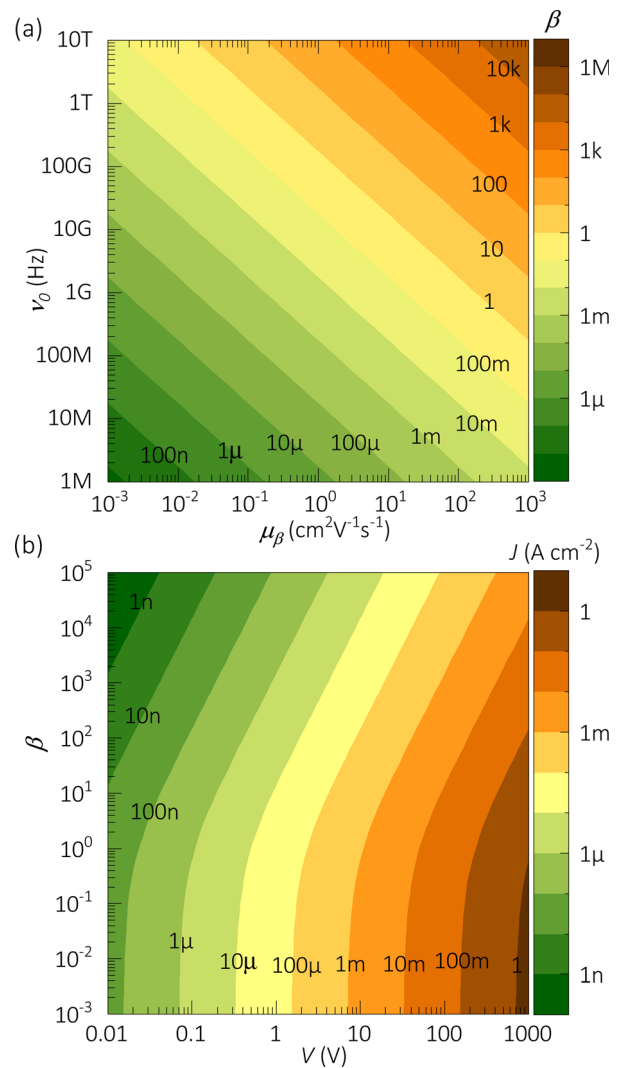
FIG. 2. The QvD-SCLCs approximation: (a) the QvD coefficient as in Eq. (3b) and (b) the current density as in Eq. (7) with $L = 1$ mm, $\epsilon_r = 23$,[16] $M = m_e$, and $Q = q$.

For $\beta \ll 2$ (e.g., low temperatures, low mobilities, and/or low effective mass charge carriers), the dissipation does not significantly affects the Child-Langmuir law[11,12] as in Eqs. (1) and (2). Thus, the use of the ballistic SCLC model would be justified with typical current values as in Fig. 1. On the other hand, the case could be a large dissipation for $\beta \gg 2$ (e.g., high temperatures, high mobilities, and/or high effective mass charge carriers). In this situation, the ballistic regime would no longer be present. In between these two limits, with $\beta \sim 2$, the QvD-SCLC would effectively modify the drift velocity as

$$v_d = \left(\sqrt{2 + \beta} - \sqrt{\beta} \right) \sqrt{\frac{Q\varphi}{M}}. \tag{4}$$

Taking the current density for the charge carrier concentration N as

$$J = Q N v_d, \tag{5}$$

one can substitute (4) and (5) in the Poisson equation[11,12]

$$\frac{d^2\varphi}{dx^2} = \frac{J}{\epsilon_0 \epsilon_r \left(\sqrt{2+\beta} - \sqrt{\beta} \right)} \sqrt{\frac{M}{Q\varphi}}, \tag{6}$$

whose solution between $x = 0$ and $x = L$, with $\varphi(0) = 0$ and $\varphi(L) = V$,[11,12] results in the QvD-SCLC current density

$$J = \frac{4\epsilon_0 \epsilon_r \left(\sqrt{2+\beta} - \sqrt{\beta} \right)}{9 L^2} \sqrt{\frac{Q}{M}} V^{3/2}. \tag{7}$$

The values from Eq. (7) are illustrated in Fig. 2(b) for electrons in a 1 mm-thick sample of MAPbI$_3$. For $\beta < 0.1$, the current is nearly that of the Child-Langmuir law, whereas it decreases as β increases.

In halide perovskites, the QvD-SCLC would be more appropriate for describing electronic kinetics due to their significantly higher mobility ($\sim 1 \, cm^{-2}V^{-1}s^{-1}$), in comparison with that of the mobile ion charge carriers ($< 10^{-6} \, cm^{-2}V^{-1}s^{-1}$). The low mobility of the ions lowers β, which makes the currents to follow the Child-Langmuir law, that could attain unrealistically large ionic currents.

The collapse of the QvD-SCLC model above presented occurs when the large dissipation ($\beta \gg 2$) produces current values out of the rage of those found in the experiment. In this case, the presence of SCLC with a $J \propto V^{3/2}$ trend could still be justified with a modified SCLC mobility regime. In the classic mobility regime, instead of relation (2), the scattering is considered and the energy dissipation for the charge carriers is parameterized with the mobility μ as

$$v_d = \mu \xi. \tag{8}$$

Similarly to the above reasoning, given a relation $v_d \propto (d\varphi/dx)^p$, one can always find a solution to the Poisson equation with a position-independent current, such as $J = \varsigma V^{p+1} L^{-p-2}$, where ς is a constant [see Eq. (S23) in Sec. S2 of the supplementary material). Thus, while $v_d \propto d\varphi/dx$ results in the Mott–Gurney law ($J \propto V^2$)[6] with a potential $\varphi \propto x^{3/2}$, a dependency, such as $v_d \propto (d\varphi/dx)^{1/2}$, implies a ballistic-like current ($J \propto V^{3/2}$) with a potential $\varphi \propto x^{5/3}$ (see Fig. 1).

For v_d to be other than linear with ξ, the mobility should be field- and, thus, voltage-dependent, which is in agreement with earlier experimental reports for halide perovskites.[19,31] Importantly, if v_d is no longer linear with ξ, the definition of mobility is no longer satisfied. Nevertheless, one can propose an effective threshold mobility μ_0 for

the transition from the Ohmic to the BVM regime of SCLC above an onset voltage V_0 so

$$\mu = \mu_0 \sqrt{\frac{V_0}{L\xi}}. \tag{9}$$

Subsequently, one can substitute Eq. (9) in (8) to obtain the BVM drift velocity

$$v_d = \mu_0 \sqrt{\frac{V_0}{L} \frac{d\varphi}{dx}}. \tag{10}$$

The conceptual ideas behind the expressions (9) and (10) are presented in Sec. S2.1 of the supplementary material under two main assumptions: (i) the larger L_i the larger μ, where L_i is Frenkel's equation[32] for the distance between the ions and their local potential maxima upon application of an external field; and (ii) the smaller L_D the larger μ, where L_D is a Debye length for the accumulation of mobile ions toward the electrodes. In addition, Eq. (10) can be deduced as a particular case of Poole-Frenkel's[9,32,33] ionized-trap-assisted transport where the charge carrier concentration is proportional to the field in a narrow bias range (see also Sec. S2.1). Summing up, it is the dual ionic-electronic conductivity of perovskites that enables the BVM regime of SCLC. The introduction of ionic space charges and mechanisms of field-dependent ionization is also suggested from the potential distribution, as presented in Fig. 1(b). The BVM model corresponds to an electrostatic potential situation somehow in between the Mott–Gurney law of SCLC (electronic bulk effect) and the quadratic case of the rectifying junctions (mobile ions depletion effect toward interfaces). Moreover, the idea of gradients in the transport properties, such as in (9), has also been proposed in the ionic dynamic doping model,[18,20,34] where the biasing produces the accumulation of mobile ions toward one electrode with slow kinetics. Consequently, one can substitute Eq. (10) in (5) to solve the Poisson equation

$$\frac{d^2\varphi}{dx^2} = \frac{J}{\epsilon_0 \epsilon_r} \sqrt{\frac{L}{\mu_0^2 V_0 \frac{d\varphi}{dx}}}, \tag{11}$$

whose solution between $x = 0$ and $x = L$, with $\varphi(0) = 0$ and $\varphi(L) = V$,[11] results in the BVM current density

$$J = \frac{\epsilon_0 \epsilon_r \mu_0}{L^3} \sqrt{2 V_0} \, V^{3/2}. \tag{12}$$

The current values for Eq. (12) are presented for a 1 mm-thick MAPbI$_3$ sample with $V_0 = 10 \, V$ in Fig. 3(a). Therefore, one can see that the BVM model results in lower currents with respect to the mobility range, in comparison with the QvD-SCLC model and the Child-Langmuir law. This suggests that the BVM regime could be appropriate for describing both electronic and ionic kinetics in halide perovskite samples. In this same direction, the time-of-flight $\tau_{tof} = L/v_d$ can be obtained by substituting Eq. (12) in (5) to obtain

$$\tau_{tof} = \frac{L^4 Q N_\tau}{\epsilon_0 \epsilon_r \mu_0 \sqrt{2 V_0}} V^{-3/2}, \tag{13}$$

where N_τ is an effective average charge carrier concentration. Typical τ_{tof} values are illustrated in Fig. 3(b) for a 1 mm-thick MAPbI$_3$ sample at 100 V. It can be seen that for single crystal samples, whose charge carrier concentration is typically lower than $10^{15} \, cm^{-3}$, the electronic
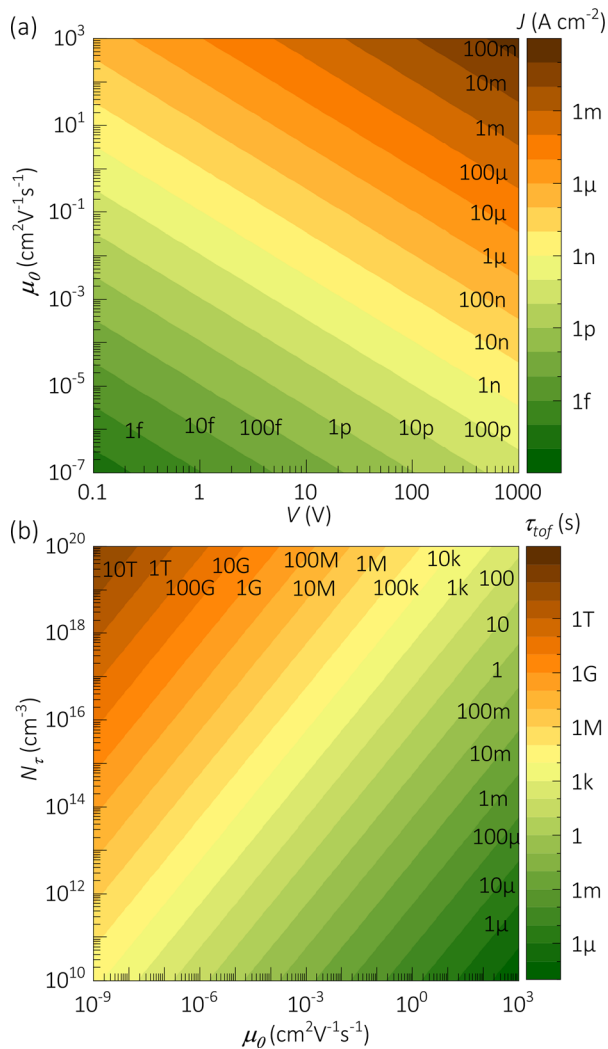
FIG. 3. The BVM regime of SCLC: (a) current density as in Eq. (12) and (b) time-of-flight at 100 V as in Eq. (13) with $L = 1$ mm, $\epsilon_r = 23$,[16] $V_0 = 10$ V.

charge carriers ($\mu_e \sim 1$ cm^{-2}V^{-1}s^{-1}) and mobile ions ($\mu_i < 10^{-5}$ cm^{-2}V^{-1}s^{-1}) would result in τ_{tof} values in the orders up to ms and ks, respectively. Purposely, a $\tau_{tof} \propto V^{-3/2}$ behavior on the order of ks has been found in our simultaneous work on 2 mm-thick MAPbBr$_3$ single crystals with measurements of long term ionic-related current transients.[21]

The definition of differential resistance $R = (dJ/dV)^{-1}$ can also be applied to the current of Eq. (12), resulting in

$$R = \frac{\sqrt{2}L^3}{3\epsilon_0\epsilon_r\mu_0\sqrt{V_0}}\, V^{-1/2}. \tag{14}$$

Experimentally, Eq. (14) relates to the resistance from impedance spectroscopy (IS) characterizations. Notably, the low frequency resistance from IS spectra has been found to behave as $R_{Lf} \propto V^{-1/2}$ in our simultaneous work on 3 mm-thick CsPbBr$_3$ single crystals.[19]

Importantly, discerning whether $J \propto V^{3/2}$ implies a QvD or a BVM regime of SCLC as Eqs. (7) and (12), respectively, can be problematic due to the experimental complications of measuring ν_0 and finding β. However, an easier approach can compare the current density behavior across a series of samples with different thicknesses. Accordingly, the linear trends $JL^2 \propto V^{3/2}$ and $JL^3 \propto V^{3/2}$ would be validating arguments for identifying QvD and BVM, respectively.

In summary, the use of the Child-Langmuir formalism of ballistic SCLC in halide perovskite has been reviewed and discussed. Our analyses suggest that even though the reports on $J \propto V^{3/2}$ are most likely artifacts due to the so-called hysteresis effect in perovskite samples, $J \propto V^{3/2}$ behaviors should not be discarded as indicators of SCLC mechanisms in halide perovskites. In this regard, two models have been introduced. A quasi-ballistic regime of SCLC was analytically presented upon the assumption of an energy dissipation proportional to the drift velocity, similar to the Stokes's drag mechanism. This model was found to most effectively describe electronic charge carrier kinetics in hybrid halide perovskites. On the other hand, we also introduced the analytical formalism for a ballistic-like mobility regime of SCLC based on a voltage dependency. By analyzing the mobility dependency of the current in this latter model, we conclude that it could well describe electronic or ionic kinetics in hybrid halide perovskite. In addition, analogous to the classic Mott–Gurney law protocols, the introduced formalisms allow the extraction of key transport parameters from the $J - V$ curve and IS spectra, such as effective values for charge carrier mobility, concentration, and time-of-flight.

See the supplementary material for the complete step-by-step deduction of the solutions of the Poisson equations and simulation.

AUTHOR DECLARATIONS

Conflict of Interest

The authors declare no conflict of interest.

DATA AVAILABILITY

The data that support the findings of this study are available from the corresponding author upon reasonable request.

REFERENCES

[1]O. Almora, D. Baran, G. C. Bazan, C. Berger, C. I. Cabrera, K. R. Catchpole, S. Erten-Ela, F. Guo, J. Hauch, A. W. Y. Ho-Baillie, T. J. Jacobsson, R. A. J. Janssen, T. Kirchartz, N. Kopidakis, Y. Li, M. A. Loi, R. R. Lunt, X. Mathew, M. D. McGehee, J. Min, D. B. Mitzi, M. K. Nazeeruddin, J. Nelson, A. F. Nogueira, U. W. Paetzold, N.-G. Park, B. P. Rand, U. Rau, H. J. Snaith, E. Unger, L. Vaillant-Roca, H.-L. Yip, and C. J. Brabec, Adv. Energy Mater. **11**, 2102526 (2021).

[2]S. Deumel, A. van Breemen, G. Gelinck, B. Peeters, J. Maas, R. Verbeek, S. Shanmugam, H. Akkerman, E. Meulenkamp, J. E. Huerdler, M. Acharya, M. García-Batlle, O. Almora, A. Guerrero, G. Garcia-Belmonte, W. Heiss, O. Schmidt, and S. F. Tedde, Nat. Electron. **4**, 681 (2021).

[3] Y. Liu, P.-A. Chen, and Y. Hu, J. Mater. Chem. C **8**, 16691 (2020).

[4] X. Xiao, J. Hu, S. Tang, K. Yan, B. Gao, H. Chen, and D. Zou, Adv. Mater. Tech. **5**, 1900914 (2020).

[5] L. Zhang, J. Miao, J. Li, and Q. Li, Adv. Funct. Mater. **30**, 2003653 (2020).

[6] N. F. Mott and R. W. Gurney, *Electronic Processes in Ionic Crystals* (Clarendon Press, 1940).

[7] K. G. Nichols and E. V. Vernon, in *Transistor Physics*, edited by K. G. Nichols and E. V. Vernon (Springer Netherlands, Dordrecht, 1966), p. 283.

[8] M. Taukeer Khan, A. Almohammedi, S. Kazim, and S. Ahmad, Chem. Rec. **20**, 452 (2020).

[9] S. M. Sze and K. K. Ng, *Physics of Semiconductor Devices*, 3rd ed. (John Wiley & Sons, Hoboken, NJ, 2007), p. 832.

[10] J. A. Röhr, D. Moia, S. A. Haque, T. Kirchartz, and J. Nelson, J. Phys.: Condens. Matter. **30**, 105901 (2018).

[11] C. D. Child, Phys. Rev. (Ser. I) **32**, 492 (1911).

[12] I. Langmuir, Phys. Rev. **2**, 450 (1913).

[13] M. S. Shur, IEEE Trans. Electron Devices **28**, 1120 (1981).

[14] J.-H. Rhew and M. S. Lundstrom, J. Appl. Phys. **92**, 5196 (2002).

[15] K. Hess and G. J. Iafrate, Proc. IEEE **76**, 519 (1988).

[16] O. Almora, A. González-Lezcano, A. Guerrero, C. J. Brabec, and G. Garcia-Belmonte, J. Appl. Phys. **128**, 075104 (2020).

[17] J. Li, X. Du, G. Niu, H. Xie, Y. Chen, Y. Yuan, Y. Gao, H. Xiao, J. Tang, A. Pan, and B. Yang, ACS Appl. Mater. Interfaces **12**, 989 (2020).

[18] M. García-Batlle, S. Deumel, J. E. Huerdler, S. F. Tedde, A. Guerrero, O. Almora, and G. Garcia-Belmonte, ACS Appl. Mater. Interfaces **13**, 35617 (2021).

[19] O. Almora, A. These, I. Levchuk, G. Garcia-Belmonte, and G. J. Matt, "Surface versus bulk currents and Ionic space-charge effects in $CsPbBr_3$ single crystals," J. Phys. Chem. Lett. submitted (2022).

[20] M. García-Batlle, O. Baussens, S. Amari, J. Zaccaro, E. Gros-Daillon, J.-M. Verilhac, A. Guerrero, and G. Garcia-Belmonte, Adv. Electron. Mater. **6**, 2000485 (2020).

[21] M. García-Batlle, J. Mayen-Guillen, M. Chapran, O. Baussens, J. Zaccaro, J.-M. Verilhac, E. GrosDaillon, A. Guerrero, O. Almora, and G. Garcia-Belmonte, "Coupling between ion drift and kinetics of electronic current transients in $MAPbBr_3$ single crystals," ACS Energy Lett. submitted (2022).

[22] E. A. Duijnstee, J. M. Ball, V. M. Le Corre, L. J. A. Koster, H. J. Snaith, and J. Lim, ACS Energy Lett. **5**, 376 (2020).

[23] E. A. Duijnstee, V. M. Le Corre, M. B. Johnston, L. Jan Anton Koster, J. Lim, and H. J. Snaith, Phys. Rev. Appl. **15**, 014006 (2021).

[24] M. S. Alvar, P. W. M. Blom, and G.-J. A. H. Wetzelaer, Nat. Commun. **11**, 4023 (2020).

[25] J. Pospisil, O. Zmeskal, S. Nespurek, J. Krajcovic, M. Weiter, and A. Kovalenko, Sci. Rep. **9**, 3332 (2019).

[26] J. Sung, C. Schnedermann, L. Ni, A. Sadhanala, R. Y. S. Chen, C. Cho, L. Priest, J. M. Lim, H.-K. Kim, B. Monserrat, P. Kukura, and A. Rao, Nat. Phys. **16**, 171 (2020).

[27] J. Sung, S. Macpherson, and A. Rao, J. Phys. Chem. Lett. **11**, 5402 (2020).

[28] Z. Guo, Y. Wan, M. Yang, J. Snaider, K. Zhu, and L. Huang, Science **356**, 59 (2017).

[29] S. L. Teitel and J. W. Wilkins, IEEE Trans. Electron Devices **30**, 150 (1983).

[30] W. Jing and M. Lundstrom, IEEE Trans. Electron Devices **50**, 1604 (2003).

[31] S. Shrestha, R. Fischer, G. J. Matt, P. Feldner, T. Michel, A. Osvet, I. Levchuk, B. Merle, S. Golkar, H. Chen, S. F. Tedde, O. Schmidt, R. Hock, M. Rührig, M. Göken, W. Heiss, G. Anton, and C. J. Brabec, Nat. Photonics **11**, 436 (2017).

[32] J. Frenkel, Phys. Rev. **54**, 647 (1938).

[33] P. N. Murgatroyd, J. Phys. D: Appl. Phys. **3**, 151 (1970).

[34] C. Li, A. Guerrero, S. Huettner, and J. Bisquert, Nat. Commun. **9**, 5113 (2018).